International Journal of Pharmaceutics 495 (2015) 362–373

Contents lists available at ScienceDirect

International Journal of Pharmaceutics

journal homepage: www.elsevier.com/locate/ijpharm

Understanding the impact of media viscosity on dissolution of a highly water soluble drug within a USP 2 mini vessel dissolution apparatus using an optical planar induced fluorescence (PLIF) method

Konstantinos Stamatopoulos[a,*], Hannah K. Batchelor[b], Federico Alberini[a], John Ramsay[a], Mark J.H. Simmons[a]

[a] School of Chemical Engineering, University of Birmingham, Edgbaston, Birmingham, B15 2TT, United Kingdom
[b] Pharmacy and Therapeutics Section, School of Clinical and Experimental Medicine, College of Medical and Dental Sciences (CMDS), Medical School Building, University of Birmingham, Edgbaston, Birmingham, B15 2TT, United Kingdom

ARTICLE INFO

Article history:
Received 13 July 2015
Received in revised form 4 September 2015
Accepted 5 September 2015
Available online 9 September 2015

Keywords:
USP 2 mini paddle
Dissolution test
Planar laser-induced fluorescence
Theophylline
Rhodamine-6G
Texture analysis

ABSTRACT

In this study, planar induced fluorescence (PLIF) was used for the first time to evaluate variability in drug dissolution data using Rhodamine-6G doped tablets within small volume USP 2 apparatus. The results were compared with tablets contained theophylline (THE) drug for conventional dissolution analysis. The impact of hydrodynamics, sampling point, dissolution media viscosity and pH were investigated to note effects on release of these two actives from the hydrophilic matrix tablets. As expected mixing performance was poor with complex and reduced velocities at the bottom of the vessel close to the tablet surface; this mixing became even worse as the viscosity of the fluid increased. The sampling point for dissolution can affect the results due to in-homogenous mixing within the vessel; this effect is exacerbated with higher viscosity dissolution fluids. The dissolution profiles of RH-6G measured via PLIF and THE measured using UV analysis were not statistically different demonstrating that RH-6G is an appropriate probe to mimic the release profile of a highly soluble drug. A linear correlation was accomplished between the release data of the drug and the dye ($R^2 > 0.9$).

The dissolution profile of the dye, obtained with the analysis of the PLIF images, can be used in order to evaluate how the viscosity and the mixing performance of USP 2 mini vessel affect the interpretation of the dissolution data of the targeted drug.

1. Introduction

A drug delivery system that provides a constant rate of release over the required time interval offers many benefits in treatment. Zero-order release provides a constant release rate and no time lag or burst effect over a prolonged time period (Yang and Fassihi, 1996). Hence, much research effort has been invested in development of zero-order oral drug delivery systems i.e. time independent release kinetics (Brazel and Peppas, 1999). The use of hydrophilic matrices has become very popular in solid oral dosage forms (Conti et al., 2007a); a sustained release matrix tablet consists of the active ingredient(s) with either single or multiple gel forming agents which retard the release of the drug (Ranga Rao and Padmalatha Devi, 1988). In the case of highly water-soluble drugs (Maderuelo et al., 2011), swelling-controlled oral drug delivery systems have so far shown the most promise.

The mechanisms by which drugs are released from a hydrophilic matrix upon hydration involve: (a) the entry of the solvent into the matrix, (b) a progressive change in the matrix from a glassy to a rubbery state resulting in swelling, (c) dissolution of the drug molecules, (d) diffusion of the drug through the gel layer and (e) release of the drug in the solution (Maderuelo et al., 2011). In the final stage, there are two phenomena which both contribute to the overall release rate of the incorporated drug: release from low viscosity gels occurs by erosion of the gel layer; whilst for high viscosity gels, the release is by diffusion of the active agent through a stable gel with limited polymer dissolution. The transition between the two mechanisms results in diffusion kinetics lying between the square root time dependence of Fickian diffusion (Korsmeyer et al., 1983) and zero-order or 'case II' diffusion (Moroni and Ghebre-Sellassie, 1995). Often, both phenomena occur simultaneously due to diffusion and the relaxation of the polymer (Zuleger and Lippold, 2001).

* Corresponding author.
E-mail address: KXS231@student.bham.ac.uk (M.J.H. Simmons).

http://dx.doi.org/10.1016/j.ijpharm.2015.09.002

Orally administered dosage forms, usually tablets, are the most convenient way for delivering drugs to patients. Upon ingestion, the tablets enter a highly dynamic environment in which disintegration, dissolution and absorption occur. This complex *in vivo* process is usually evaluated *in vitro* using disintegration and dissolution tests. In the case of hydrophilic matrices, the timescale for gel formation and the resistance of the gel layer to physiological shear stress, experienced during their passage through the gastrointestinal (GI) tract, are essential parameters that control the drug dissolution characteristics (Garbacz et al., 2009). Thus, different types of dissolution apparatus have been developed to reproduce the mechanical stresses present within the GI tract.

Recently, the small volume USP 2 apparatus has gained popularity due to the reduced mass of material requried, analytical methodology and discriminatory power of conventional apparatus. Furthermore, small volume apparatus may be beneficial in the development of biorelevant methods, particularly for paediatric populations.

Officially introduced almost 4 decades ago, the conventional (1 L) USP dissolution Testing Apparatus 2 (USP 2) is the most commonly used equipment in the pharmaceutical industry (Mitchell et al., 1993a; Zuleger et al., 2002). However, this apparatus presents some drawbacks (Bai et al., 2011). Numerous published works have indicated that there is high variability in dissolution profiles using USP 2 (Baxter et al., 2005a; Costa and Lobo, 2001; Kukura et al., 2003; Qureshi and McGilveray, 1999; Qureshi and Shabnam, 2001).

Some studies (Baxter et al., 2005a; Kukura et al., 2004; Zuleger et al., 2002) have shown that the fluid flow in USP 2 is highly heterogeneous. The shear distribution is non-uniform (Kukura et al., 2004), whereas, the velocity vectors are highly dependent on the location within the vessel, especially at the bottom of the vessel where the tablet is located during dissolution testing (Zuleger et al., 2002). These complex hydrodynamics can contribute to the poor reproducibility, as can the tablet position in the vessel. The small volume USP 2 apparatus is a miniaturised version of the conventional apparatus, however, there is still a need to analyze the hydrodynamics since the miniaturised systems do not exactly reflect the conditions of the standard paddle system (Klein and Shah, 2008), nor the conditions in the GI tract.

The effect of viscosity on the dissolution test may increase the uncertainty and the variability of the results, since, the hydrodynamics of the USP 2 apparatus will be more complicated. In addition, other variables, like sampling cannula position, especially sampling depth, and inconsistencies in the technique of the analysts performing the test can affect dissolution rate and reproducibility (Gray et al., 2009). Previous works (Parojcic et al., 2008; Radwan et al., 2012) testing different dosage forms in viscous media do not give any information about the sampling cannula position or possible changes in hydrodynamics (e.g., shear rates and/or velocities) or mixing patterns.

Planar Induced Fluorecence (PLIF) has been widely used as a non-intrusive visualization technique for the evaluation of mixing systems (Bruchhausen et al., 2005; Law and Wang, 2000; van Cruyningen et al., 1990). Furthermore, Particle Image Velocimetry (PIV) combined with computational fluid dynamics (CFD) have been used to characterize the flow pattern in conventional (1 L) USP 2 apparatus dissolution vessel (Baxter et al., 2005a; Kukura et al., 2003), revealing the non-uniform velocity field and thus an uneven distribution shear rates.

These visualization techniques have mainly been used either by injecting a fluorescent dye in the USP 2 vessel, at different injection points, for characterising mixing patterns in simple buffer solution (Baxter et al., 2005a; Kukura et al., 2004) or by using non-disintegrating salicylic acid containing phenolphthalein as an indicator agent for investigating the effect of tablet movements at the bottom of the vessel on drug dissolution profiles (Baxter et al., 2005a,b). In addition, visualization studies were performed by blending salicylic acid with phenolphthalein as a first step in affirming the fluid flow patterns in USP 1 and 2 (Mauger et al., 2003), demonstrated previously using laser Doppler anemometry (Bocanegra et al., 1990).

Kukura et al. (2003, 2004) performed PLIF experiments in conventional (1 L) USP 2 dissolution apparatus under laminar and turbulent conditions. Under laminar flow ($Re = 150$) non-uniform mixing with segregation zones were observed due to the failure of dye to reach the upper regions of the dissolution vessel. In case of turbulent flow ($Re = 5000$) the authors could not find a significant difference in dissolution profiles of the targeted drug at the different sampling points, although, large fluctuations of the mixing patterns were observed with time. This contradiction might be due to the fact that the PLIF method is capable of capturing local time-dependent mixing conditions in the USP 2 apparatus which are not observable with the conventional sampling technique. Furthemore, Kukura et al. (2003, 2004) did not repeat the experiment for low *Re* numbers and compare the PLIF results with those from dissolution experiments.

It is important to understand whether variability in dissolution is due to the manufacturing process of the dosage form, leading to a burst effect from sustained release formulations, especially when highly water soluble drugs are presented in high amounts (Gray et al., 2009); or due to the dissolution testing method, e.g., physicochemical properties of the media (e.g., viscosity) with direct effect on hydrodynamics of the USP 2 dissolution apparatus.

Whilst PLIF and other visualisation techniques such as PIV have been used to previously evaluate the drawbacks of the USP 2 dissolution apparatus (Baxter et al., 2005a; Kukura et al., 2003, 2004), they do not allow any direct or indirect correlation with the dissolution profile of the active compound, since the form of PLIF used involved injecting fluorescent dye at different points inside the USP 2 vessel, rather than dye release from a tablet. Due to the complexity of the hydrodynamics and mixing intensity in the vessel, a PLIF method which incorporates a fluorescent dye into a hydrophilic matrix (which can mimic the dissolution profile of a highly water soluble drug) and then tracks the release through the vessel over time overcomes these limitations.

Thus, in this paper, PLIF has been utilized as a non-intrusive method for visualizing the mixing patterns and quantifying the local concentrations of RH-6G) released from a hydrophilic matrix that also contained the targeted drug. Thus, indirect evaluation of the impact of the hydrodynamics, viscosity and sampling point on the dissolution of the drug has been performed. A correlation of the dissolution experiments of the RH-6G using PLIF with those of the targeted drug using the conventional analytical technique is presented. This work, coupled with the texture analysis of the hydrophilic matrix, gives an overview of the critical parameters affecting the interpretation of the dissolution results. Theophylline (THE) was selected as a well-known, highly soluble drug where extensive *in vitro* dissolution data from hydrophilic matrices is readily available. As mentioned above, the USP 2 small volume (100 mL) dissolution apparatus was chosen as an alternative to the standard paddle set up, as this apparatus has not previously been investigated.

2. Materials and methods

2.1. Materials

Sodium carboxymethylcellulose of 90000 ($NaCMC_{90000}$) and 700000 ($NaCMC_{700000}$) molecular weight was purchased from Sigma (St., Louis, USA). Theophylline anhydrous and potato starch were bought from Acros Organics (Loughborough, UK). Sodium

hydroxide, Rhodamine-6G, hydrochloric acid (1 M), silicone dioxide and potassium hydrogen (KH_2PO_4)- and dihydrogen phosphate (K_2HPO_4) were purchased from Sigma (St., Louis, USA).

2.2. Fluids and fluid properties

$NaCMC_{700000}$ was selected as a chemically inert, water-soluble polymer which can mimic the shear thinning rheology of the chyme. $NaCMC_{700000}$ buffered solutions of 0.25, 0.5 and 0.75% (w/w) were prepared using 0.05 M phosphate buffer pH 7.4 (KH_2PO_4/K_2HPO_4). This pH value was selected as a representative pH for the large intestine. All the tested fluids were deaerated using an ultrasound bath before conducting dissolution and PLIF experiments.

The rheology of the NaCMC solutions was measured using a Discovery Hybrid Rheometer (TA Instruments—a division of Waters Ltd.) coupled with a 40 mm diameter, 4° cone and plate geometry. The temperature was controlled to 37 °C using an in-built Peltier plate (at the same temperature as the USP 2 experiments). The rheology was obtained by performing a shear ramp over a range of shear rate from 0.1–1000 s^{-1}. The data was found to fit the Herschel–Bulkley model.

$$\tau = \tau_Y + K\dot{\gamma}^n \quad (1)$$

Where τ is the shear stress, τ_Y is the yield stress $\dot{\gamma}$ is the shear rate, K is the consistency index and n is the power law exponent. The apparent viscosity, μ_A, can be thus determined by evaluating $\tau/\dot{\gamma}$ at a given value of shear rate. The rheological properties of the experimental fluids are presented in Table 1.

2.3. Tablet preparation

A 500 mg tablet was prepared according to the following composition: 50% THE, 44.1% $NaCMC_{90000}$, 4.9% potato starch and 1% silicone dioxide. The powders were sieved and mixed for 10 min then placed into a single die tableting machine (Kilian, Coln, D) fitted with flat-faced 9.8 mm punches and instrumented with piezoelectric load washer (Kistler,Winterthur, CH) to enable compression force measurements. To investigate the effect of the compression load and compression time on dissolution profile of drug from the tablet, a load pressure range of 980.6–1961.2 bars for 20 and 40 s was applied. The cylindrical tablets had a final weight of 500 ± 25 mg. The same method was followed for the tablets used in PLIF experiments containing 0.02% RH-6G. Fig. 1a shows pictures of the different tablets used in dissolution, PIV and PLIF experiments. For the PIV experiments, a piece of acrylic cut to match the dimensions of the tablet was used to enable monitoring of the flow above the surface of the tablet.

2.4. Experimental apparatus: USP 2 mini paddle

A schematic of the USP 2 mini paddle dissolution apparatus (Dissolution Tester 6000, Antech, UK) is shown in Fig. 1b. The volume of media used in all experiments was 100 mL and the paddle rotational speed was fixed at 50 rpm. The same apparatus

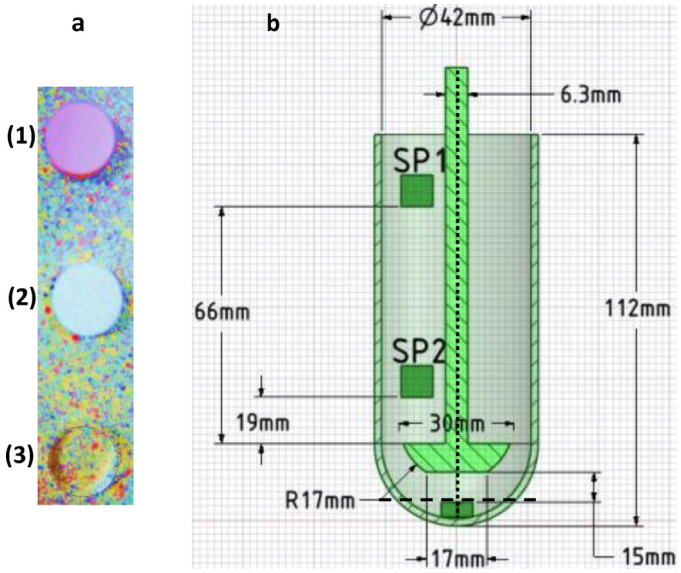

Fig. 1. (a) The three tablets used in: (1) PLIF (containing RH-6G), (2) dissolution tests and (3) PIV experiments (acrylic); (b) Dimensions of the USP II mini vessel used in dissolution, PIV, PLIF experiments indicating the two sampling areas (SP1 and SP2) as well as the horizontal (----) and vertical plane (·····) that laser cut the vessel in PIV experiments.

was used for (i) dissolution (ii) PLIF and (iii) PIV studies. All the experiments were performed at 37 °C. The flow regime in the vessel was determined by calculation of the Reynolds number

$$Re = \frac{\rho N D^2}{\mu_A} \quad (2)$$

where ρ is the fluid density, N is the rotational speed, D is the impeller diameter. The apparent viscosity, μ_A, was estimated using the Metzner-Otto method (Metzner and Otto, 1957) which assumes the shear rate in the vessel is proportional to the impeller speed, thus

$$\mu_A = \frac{\tau_Y}{k_S N} + K(k_S N)^{n-1} \quad (3)$$

The value of Metzner-Otto constant,k_S, in the above expression was 10. The calculated values of Re are given in Table 1.

2.5. Dissolution experiments

Dissolution tests (six replicates) were performed in 0.1N HCl solution (gastric conditions) and in 0.05 M phosphate buffer solution (pH 7.4) corresponding to large intestine conditions. The dissolution tests for the viscous media were conducted only at pH 7.4; assuming that viscosity increases as the dewatering of the chyme takes place in large intestine. Two sampling positions were selected (Fig. 1b), denoted SP1 and SP2, located at a distance of 66 mm and 20 mm from the paddle blade, respectively. Samples of 1 mL volume were withdrawn at predetermined time intervals (5,

Table 1
Rheological characteristics of the dissolution media employed; ρ :density (kg m^{-3}), τ_Y : yield stress (Pa), μ_A : apparent viscosity (mPa s), k : proportionality constant related to the structural and geometrical properties of the matrix, Re: Reynolds number and $\boldsymbol{m}$ is the diffusional exponent indicative of the drug release mechanism.

	ρ(K gm^3)	τ_λ(Pa)	μ_A(mPas)	k	m	Re	Regime
"Simple" buffer	1000.1		1		1	1503	Transitional
0.25% NaCMC (w/w)	1017.6	0.03	13.34	0.044	0.58	114.6	
0.50% NaCMC (w/w)	1020.4	0.18	98.11	0.229	0.72	17.6	
0.75% NaCMC (w/w)	1024.5	0.76	575.6	0.83	0.85	2.6	Laminar

10, 15, 30, 60, 120, 240, 480, 560 min and the last one after completing 21 h dissolution testing). The volume of the medium removed at each time point was replaced with fresh media. Each sample was filtered using a 0.4 μm PTFE filter (Ghori et al., 2015) and appropriately diluted prior to quantitative analysis in order to be within the linear region of the calibration curve Eq. (2). Quantitative analysis of theophylline was undertaken using a UV spectrophotometer (Jenway Genova Plus) at 270 nm.

A calibration curve was obtained by plotting the absorbance of the theophylline at 270 nm versus the concentration (mg L^{-1}). For this purpose standard solutions of theophylline were prepared at several concentration intervals (2, 5, 10, 20, 40 mg L^{-1}).

$$y = 0.0575x - 0.0024 \quad (R^2 = 0.9987) \tag{4}$$

The dissolution data obtained as a function of time were fitted to the following equation Eq. (4) which is widely used to describe the drug release behaviour from hydrophilic polymeric matrices (Conti et al., 2007b; Korsmeyer et al., 1983).

$$\frac{M_t}{M_\infty} = kt^m \tag{5}$$

where M_t/M_∞ is the fraction of drug released at time t,k is the proportionality constant related to the structural and geometrical properties of the matrix, and m is the diffusional exponent indicative of the drug release mechanism. The exponent, m, is strongly dependent upon relaxation rate at the swelling front and the polymer swelling characters. As this equation is valid only for the early stages (<70%) of drug release, it was only fitted to values of $M_t/M_\infty < 0.7$.

2.6. PIV and PLIF studies

Both PIV and PLIF studies were carried out using a TSI PIV system comprised of a 532 nm Nd-YAG laser (Litron NanoPIV) pulsing at 7.4 Hz, and a single TSI Powerview 4MP (2048 × 2048 pixels) 12 bit frame-straddling CCD camera, both controlled using a synchronizer (TSI 610,035) attached to a personal computer equipped with TSI Insight 4G software. The spatial resolution of the measurements was 10 μm $pixel^{-1}$. The small volume USP 2 vessel was placed in a glass box filled with water which served the dual purpose of eliminating refractive index issues due to vessel curvature and also in enabling temperature to be kept constant at 37 °C by circulating the fluid in the box through a water bath using a peristaltic pump. The laser sheet was aligned vertically, passing across the diameter of the vessel, i.e. aligned with the impeller shaft along the vessel axis.

PIV experiments were carried out by seeding the fluid with 10 μm silver coated particles (Dantec Inc, DU) which possess a sufficiently small relaxation time to be able to follow the fluid streamlines (Gabriele et al., 2009). 500 image pairs were recorded for each experiment and the average flow fields obtained using the TSI Insight and Tecplot Focus 2013 software (Tecplot Inc., USA).

For the PLIF experiments, a cut-off filter at 545 nm was fitted to the CCD camera to eliminate reflected laser light and to capture only the fluorescent light emitted by the RH-6G (λ = 560 nm). The system was calibrated for each solution used at fixed laser power by filling the USP 2100 mL (small volume) vessel with well mixed solutions at concentrations ranging 0–1.0 mg L^{-1}; in steps of 0.1 mg L^{-1}. 50 images were captured at each concentration to enable the variation of laser power upon the resultant grayscale

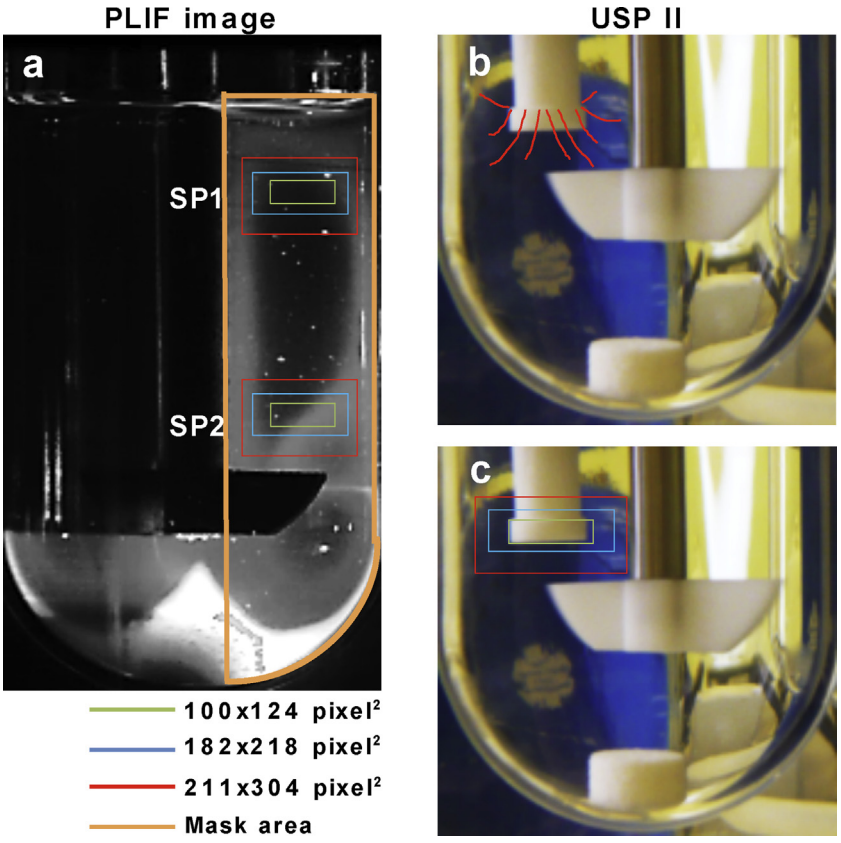

Fig. 2. (a) Schematic representation of the sampling point and size selected within the mask area of PLIF images corresponding to the cannula position in USP 2 mini vessel dissolution apparatus; (b) Red streamlines illustrate the pumped material by the cannula around its filter diameter and (c) the corresponding theoretical sampling area selected for processing PLIF images.

values in the image to be obtained. The relative standard deviation in values was consistently less than 3.6% and therefore not significant. A mask was set as shown in Fig. 2a to consider only half of the illuminated tank, up to the vessel axis (the remainder being in shadow due to impingement of the laser sheet on the impeller shaft). The calibration was developed by taking the average grayscale values over the 50 images, then on a pixel by pixel basis and performing a linear regression over two concentration ranges from 0–0.6 mg L^{-1} and 0.6–1.0 mg L^{-1}, respectively. This was due to quenching phenomena which occurred for RH-6G concentrations >0.6 mg L^{-1}. The amount of RH-6G in the tablet was chosen such that the final concentration in the dissolution vessel was 1 mg L^{-1} ensuring all values were below the saturation signal of the CCD camera used in PLIF experiments. In addition, 1 mg L^{-1} was also the proper amount for the establishment of sink conditions. The analysis was carried out using MATLAB (Matlab 7.6.0 R2008a) to produce calibration matrix.

$$\underline{\underline{C}} = \underline{\underline{A}}\,\underline{\underline{G}} + \underline{\underline{B}} \quad (6)$$

where $\underline{\underline{C}}$ is the concentration matrix, $\underline{\underline{A}}$ is the matrix of constant vales, $\underline{\underline{G}}$ is the matrix of averaged Grayscale values and $\underline{\underline{B}}$ is the matrix of intercept values for the linear regression. The regression was carried out using a standard least-squares method.

The PLIF measurements were conducted by addition of the RH-6G tablet into the bottom of the vessel, and following the same dissolution protocol (Section 2.5). 10 images were recorded at each predetermined time interval. Following post-processing using the calibration matrix, two interrogation regions were selected matching the sampling points used in the dissolution experiments (SP1 and SP2). Assuming that during the sampling process in dissolution experiments, the cannula might draw material from a wider area (Fig. 2b), three different sampling point areas were considered of 100×124, 182×218 and 211×304 pixels respectively (Fig. 2c). Average values of concentration as a function of time and as a function of the two sampling areas (SP1 and SP2) were thus obtained to enable direct comparison with the theophylline dissolution tests described in Section 2.5.

2.7. Gel layer strength and thickness measurements

Tablets with and without RH-6G were placed in two solutions with different values of pH (1.0 and 7.4), and the impeller speed and the operation temperature were set as described in Section 2.4. In order to avoid deformation during the analysis, one planar base of the tablets was stuck to a metal flat base. The swollen tablets were removed from the dissolution apparatus after 1.0, 2.0 and 5.5 h for texture analysis. The strength and thickness of the gel layer, during swelling process, was tested in triplicate using a Texture Analyzer (TA.XT2, Stable Micro System, Goldalming, UK), which provided force-time curves recorded during the penetration process. The penetration of a flat-tipped round steel probe (4 mm diameter and 30 mm length) into swollen matrices was determined at a constant speed of 0.1 mm s^{-1}, under increasing load. Data collection and analyses were performed by a computer equipped with Texture Expert® software. A predetermined maximum penetration of 3 mm was established in order to prevent the contact of the probe with the glassy core.

2.8. Statistical analysis

Comparison of the dissolution profiles of THE and RH-6G was conducted using model-dependent and model-independent methods. Differences between the two sampling points for both dissolution tests (i.e., conventional USP 2 and PLIF) as well as the size of the sampling area in PLIF images, were tested for significance using ANOVA with a value of $p < 0.05$. The release rate mechanism in the simple buffer at both pH used (i.e., 1.0 and 7.4) was determined using Korsmeyer–Peppas fitting model as described in Eq. (5). The similarity between dissolution curves of THE and RH-6G, obtained in different viscous media, was tested by the f_2-statistic (Eq. (7)) where f_2 value between 50 and 100 suggests that two dissolution profiles are similar (Radwan

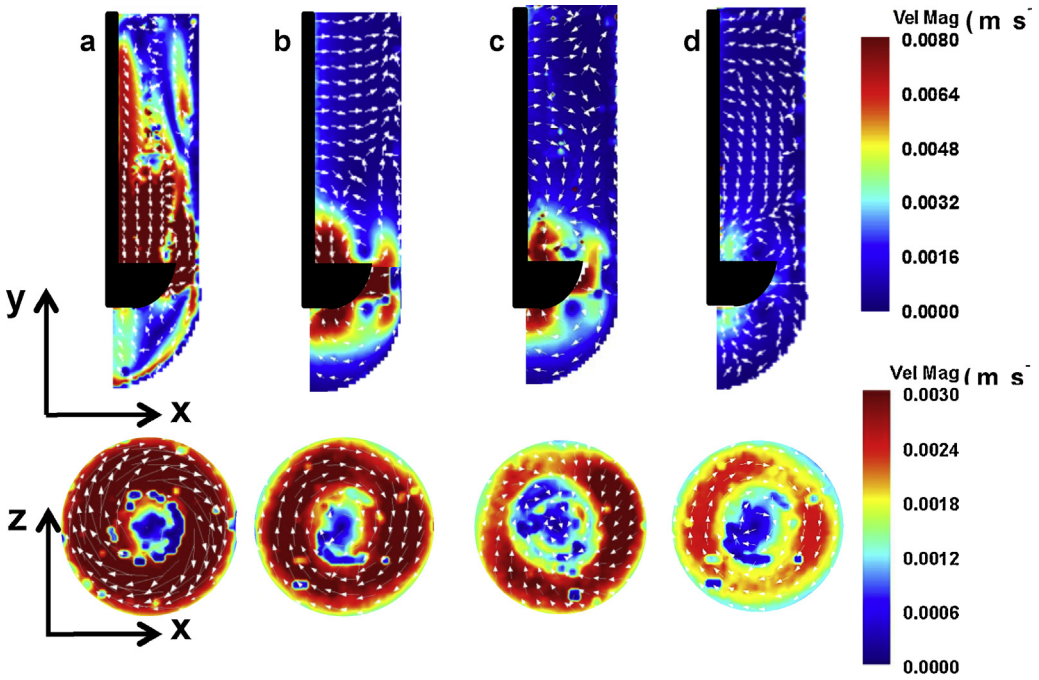

Fig. 3. Time average velocity fields measurements in vertical USP II mini vessel (top) and horizontal section (bottom) above the tablet surface for: (a) water($Re = 1503.0$), (b) 0.25% NaCMC (w/w) ($Re = 114.64$), (c) 0.5% NaCMC (w/w) ($Re = 17.63$) and (d) 0.75% NaCMC (w/w) ($Re = 2.67$) NaCMC (w/w). The units of velocity magnitude are m s^{-1}. Impeller speed: 0.785 m s^{-1} and operation temperature 37 °C.

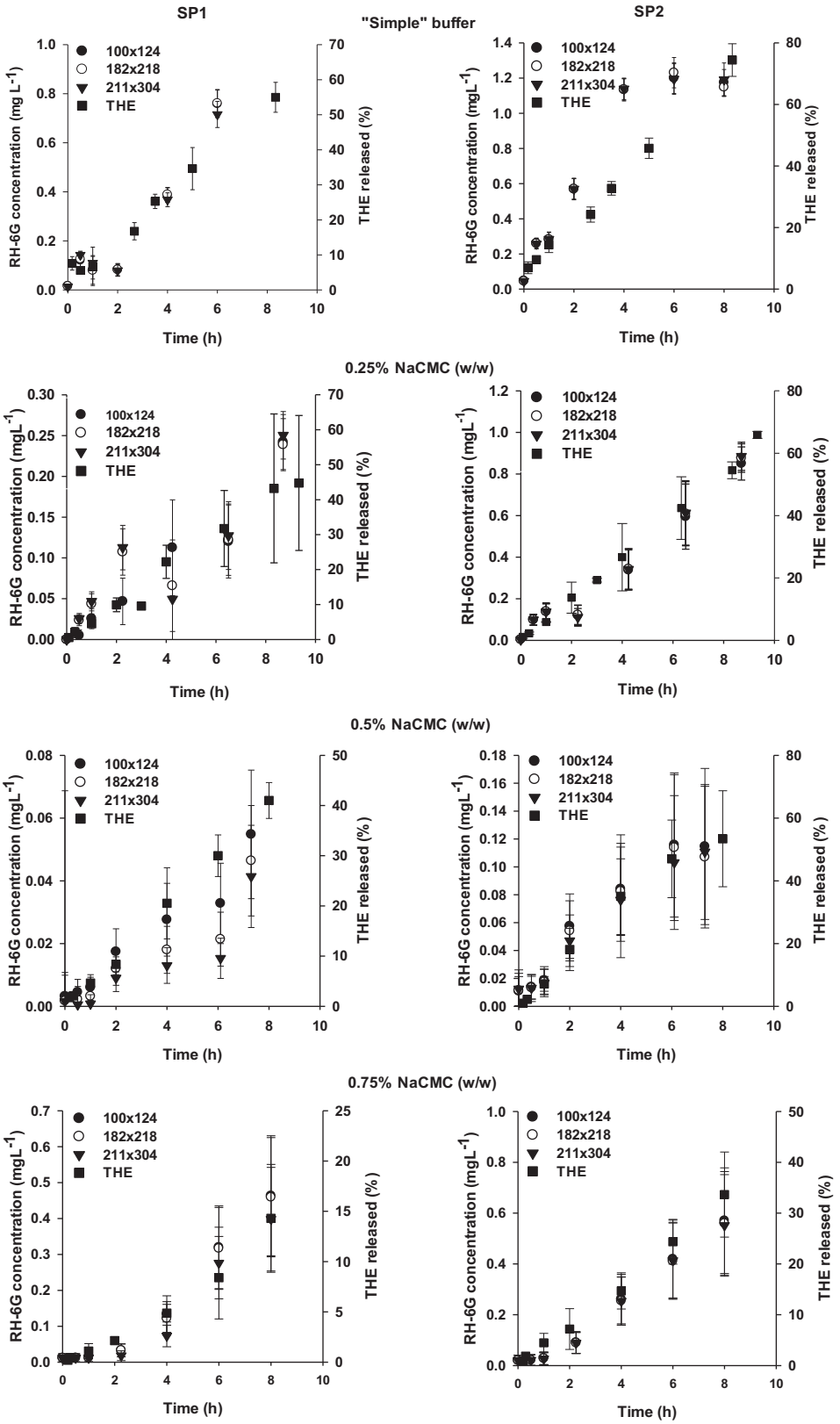

Fig. 4. Effect of size of the sampling area on the interpretation of the dissolution data of RH-6G obtained from PLIF images and comparison with theophylline (THE) release profile obtained at sampling point 1 (SP1) and sampling point 2 (SP2) in different viscous media. The legend entries refer to sample size (● 100 × 124, ○ 182 × 218 and ▼ 211 × 304) for the RH-6G profile and the release profile (■) of theophylline (THE). Standard deviation bars for RH-6G ($n = 10$) and THE ($n = 6$).

et al., 2012).

$$f_2 = 50 * log\left[\frac{100}{1+\sqrt{\frac{\sum_{t=1}^{t=n}(R_t - T_t)^2}{n}}}\right] \quad (7)$$

R_t = Dissolution (%) for drug formulation at time t

T_t = Dissolution (%) for dye formulation at time t

n = number of time points

The concentration values of RH-6G were normalized (% release) before calculating the similarity factor. In addition, mean dissolution time (MDT) was calculated as model-independent parameter describing kinetics of drug and dye dissolution under various viscous media (Eq. (8)).

$$\text{MDT} = \frac{\sum_i \bar{t}\Delta M_i}{\sum_i \Delta M_i} \quad (8)$$

where: $\bar{t}_i$ is the central point of the observed time interval and $\Delta M_i$is the differential amount of drug dissolved.

Finally, linear regression of the dissolution data of THE and the RH-6G obtained under the experimental conditions was performed.

3. Results

3.1. Effect of compression load and time on dissolution profile of theophylline

When manufacturing hydrophilic matrices by direct compression is very important to take into consideration the load and the speed of the compression process (Maderuelo et al., 2011), since variations in the compression force can affect subsequent drug release when a low viscosity grade polymer is used (Hiremath and Saha, 2008). Hence, two different compression pressures and two different compression times were tested in order to evaluate the impact on the dissolution profile of THE since a low viscosity grade $NaCMC_{90000}$ was used. The dissolution data of THE obtained at compression pressures of 980.6 bar and 1961.2 bar respectively, showed no influence of compression time on the release of the THE. These results are consistent with works from other authors working on hydrophilic matrices who found either a very slight reduction in drug release (Ebube et al., 1997) or no significant effect (Ford et al., 1987; Khanvilkar et al., 2002; Mitchell et al., 1993b). Thus, for the following THE and RH-6G dissolution tests, compression pressures and time were fixed at 980.6 bar and 20 s respectively.

3.2. Particle image velocimetry (PIV)

Fig. 3 shows the time average velocity fields ($m\,s^{-1}$) measured by PIV experiments in water and three different viscous NaCMC media. In all experimental fluids the maximum time average velocity was 10% (0.008 $m\,s^{-1}$) of the paddle speed (0.08 $m\,s^{-1}$). Each subfigure shows the spatial distribution of the time average velocity in the vertical plane of the impeller (top) and in the transverse cross section of the mini vessel at the top surface of the tablet (bottom). Based on the calculated Reynolds numbers (Table 1) the results span both transitional ('simple' buffer, 0.25% and 0.50% NaCMC w/w) and laminar (0.75% NaCMC w/w) regimes. In case of the viscous media, the most intense motion takes place mainly around the impeller, whereas away from the impeller blades the flow slows and becomes almost stagnant. In the vertical, two circulation zones were observed with clockwise (below the blade) counter- clockwise (above the blade) flowing pattern. As the viscosity is increased the circulation loop becomes smaller with reduced velocities in the most viscous medium (i.e., 0.75% NaCMC w/w) shown in Fig. 3d. However, relatively high velocities were observed close to blade and the shaft corner and below the blade compared to the flow away from this area. In the 'simple' buffer (water), another loop was detected at the top of the vessel where the sampler was located (sampling point 1; SP1) forming a second mixing area. This was not observed in the viscous media. The velocity vectors indicate, except for the 0.25% NaCMC (w/w), that there was a downward flow starting from the top region of the vessel to the blade. In contrast, for the 0.25% NaCMC (w/w) (Fig. 3b), an upward flow pattern was observed close to the wall which extended from the tip to the top region of the vessel. In addition, the velocities vectors showed that the flow, outside the circulation zone and parallel to the blade, had a direction from the shaft to the wall encountering the upward flow pattern coming from the tip. This flow pattern differs from 0.5% and 0.75% NaCMC (w/w), possible due to fluid motion generated by the shaft rotation. The effect of the shaft rotation seems to be inefficient in order to generate fluid motion in the more viscous media; i.e., 0.5% and 0.75% NaCMC (w/w).

The flow fields in the transverse sections in Fig. 3 (bottom) illustrate the presence of a circular low velocity region located at the vessel axis above the tablet surface. The maximum velocity was 3.75% (0.003 $m\,s^{-1}$) of the paddle speed, although, in 0.75% NaCMC was below 0.0024 $m\,s^{-1}$ (<3%). This region is extended from the tablet surface to the lowest point of the shaft and is critical to the performance of the dissolution test (Bai et al., 2011), since it defines the shear forces applied on the surface of the hydrophilic matrix and hence the erosion of the gel layer. Therefore the drug release will be strongly influenced by the hydrodynamics in this region. This region increases in size, becoming larger than the tablet diameter, as the viscosity increases. These observations are in accordance with the previous studies illustrating the poor mixing performance of USP 2 dissolution apparatus and the complex and reduced velocities within the bottom area in which where the tablet is placed (Baxter et al., 2005a, b; Kukura et al., 2004; Zuleger et al., 2002).

3.3. Drug and RH-6G dissolution and release kinetics

Fig. 4 shows the effect of the sampling point and the size of the sampling area on the dissolution profile of RH-6G obtained from the PLIF and comparison with the profile of theophylline (released %). The results showed for SP2 that the average concentration values of the RH-6G (mgL^{-1}), were not statistically different ($p > 0.05$) between each of the three different sample sizes (100×124, 182×218, 211×304; $pixel^2$) for all the experimental fluids. However, in case of 0.25%, 0.5% NaCMC (w/w), the average value of dye concentration was found to decrease as the size of the sampling area was increased for the SP1. This was due to the fact that in the large sampling size more low concentration values were included from the dead zones resulting in a decrease of the average value. Nevertheless, the standard deviations bars are overlapped implying no statistically significant difference.

In addition, as the sampling size and the viscosity of the fluid were increased, the coefficient of variance (C.V) also increased. The C.V for the simple buffer lay between 5–10% for SP2 as the sampling area increases from 100×124 to 211×304 $pixel^2$. Higher values of C.V were observed (22–29%) for the corresponding results at SP1. The viscosity of the fluid had a significant impact on the concentration variability of RH-6G within the selected sampling area and especially in SP1. In case of 0.25% NaCMC (w/w), C.V values ranged 32.6–52.6% and 7.2–26.5% for SP1 and SP2, respectively. Even higher C.V values were observed in 0.5% NaCMC (w/w). In particular, C.V values for SP1 and SP2 were 44.6–46.6%

Table 2
Distribution of the RH-6G (average concentration ($mg\,L^{-1}$)) throughout the USP 2 mini vessel in different viscous media.

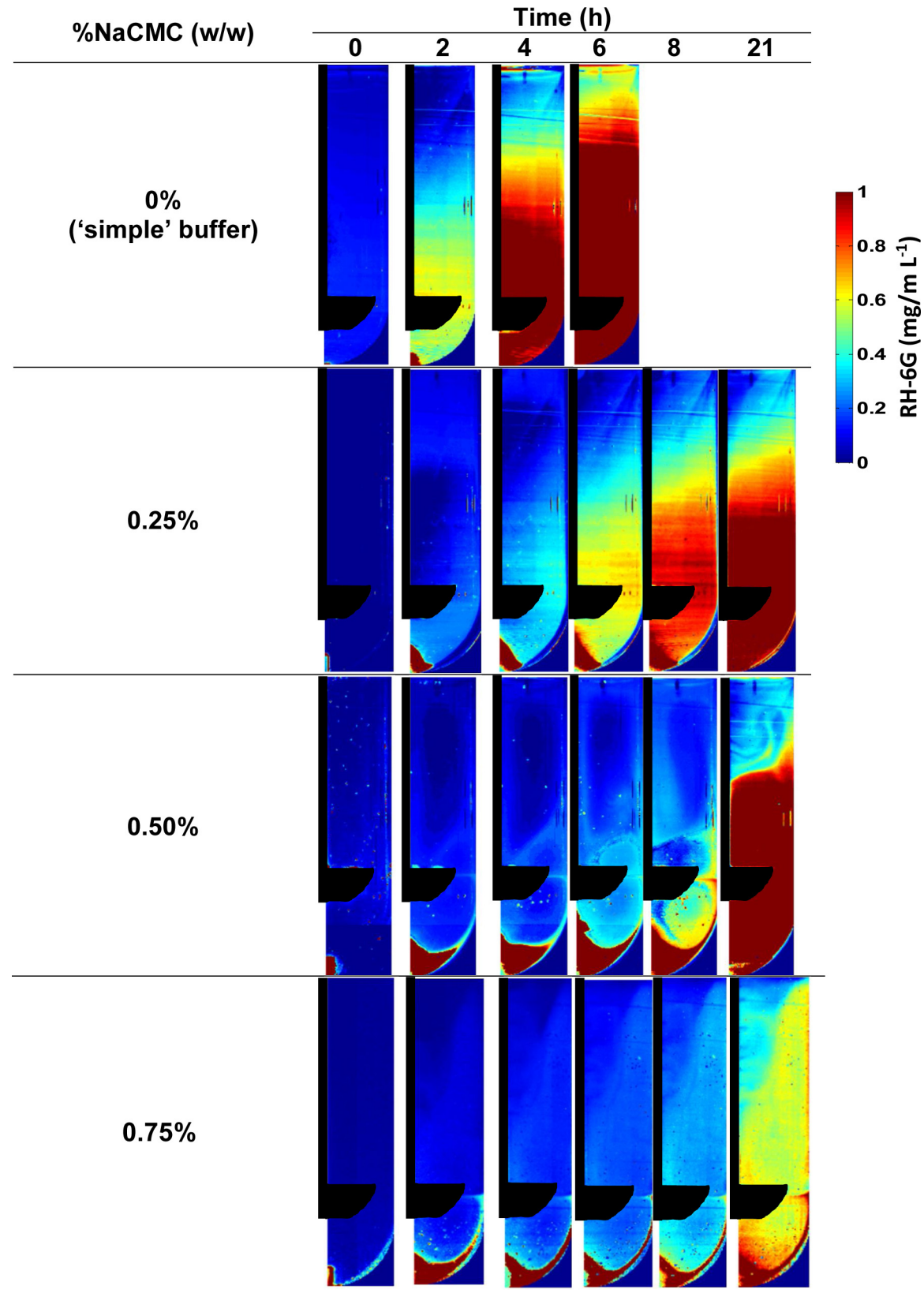

Table 3
Comparison of the release kinetic mechanism of theophylline and Rhodamine-6G from hydrophilic matrix under different experimental fluids, using model-dependent and –independent parameters.

	Simple buffer				%NaCMC (w/w)[a]					
	pH 1.0		pH 7.4		0.25		0.5		0.75	
	USP	PLIF	USP	PLIF	USP	PLIF	USP	PLIF	USP	PLIF
	–		–		–		–		–	
	SP2 = 35.9		SP2 = 55.2		SP2 = 51.9		–		–	
	51.0[b]	32.7[b]	52.6[b]	30.9[b]	46.8[b]	30.8[b]	–	–	–	–
MDT[c]	3.82	3.9	3.12	2.97	4.13	4.2	4.41	4.3	4.94	4.77
m[d]	0.75 – 0.82	0.57 – 0.61	1.46 – 1.52	1.24 – 1.33						
R^2	0.985	0.993	0.992	0.941						

[a] 0.05M phosphate buffer (pH 7.4).
[b] values obtained by comparing SP1 and SP2 dissolution data of theophylline and RH-6G separately.
[c] Mean dissolution time (MDT).
[d] the lowest values were obtained from fitting the dissolution data of sampling point 1 (SP1) whereas the highest values are for the sampling point 2 (SP2).

and 39.2–41% respectively, whereas in 0.75% NaCMC (w/w), were 37.2–45.8% (SP1) and 38.4–42% (SP2).

Furthermore, a faster release profile was obtained for both compounds based on SP2 data, compare to the corresponding SP1 one.

Table 2 presents the local colour scaled concentration values of RH-6G throughout the mini vessel as a function of dissolution time, under different experimental fluids. The main observations are that: (a) the concentration of the dye was always higher around the blade, in contrast to the upper region, explaining the faster release rate observed based on SP2 compare to SP1 (Fig. 4), (b) as the viscosity is increased dead zones and high fluctuations in the distribution of the dye was occurred, revealing the high C.V values obtained in viscous media, (c) in the most viscous media (i.e., 0.50% and 0.75%) the dye accumulates at the bottom of the vessel before it reaches the upper region of the vessel. These results can explain the high standard deviation observed in theophylline release data and the dissimilarities in the dissolution profiles between SP1 and SP2. Comparison of RH-6G and THE dissolution profile was not possible with using the similarity factor (f_2) (Table 3) for those cases where C.V was >10%. Nevertheless, the standard deviation bars of THE data points and those of RH-6G (Fig. 4) overlapped; implying that from statistical point of view there was no a significant difference. Failure of obtaining$f_2 > 50$, in case of pH 1.0 for SP2, might be to due burst release upon hydration of the tablet in 0.1N HCl solution. Similar effects were noted by (Conti et al., 2007a). In this case, the gel hydration rate is slower and the dye molecules present at the surface of the tablet can dissolve and pass into the fluid; the solubility of RH-6G is 20 mg mL^{-1} @ 23 °C compared to THE which is 8.3 mg mL^{-1}. However, sink conditions, defined as having a volume of medium at least three times the volume required to form a saturated solution of drug substance, are present in both cases which ensures that the dissolution test reflects the properties of the dosage form and not the drug

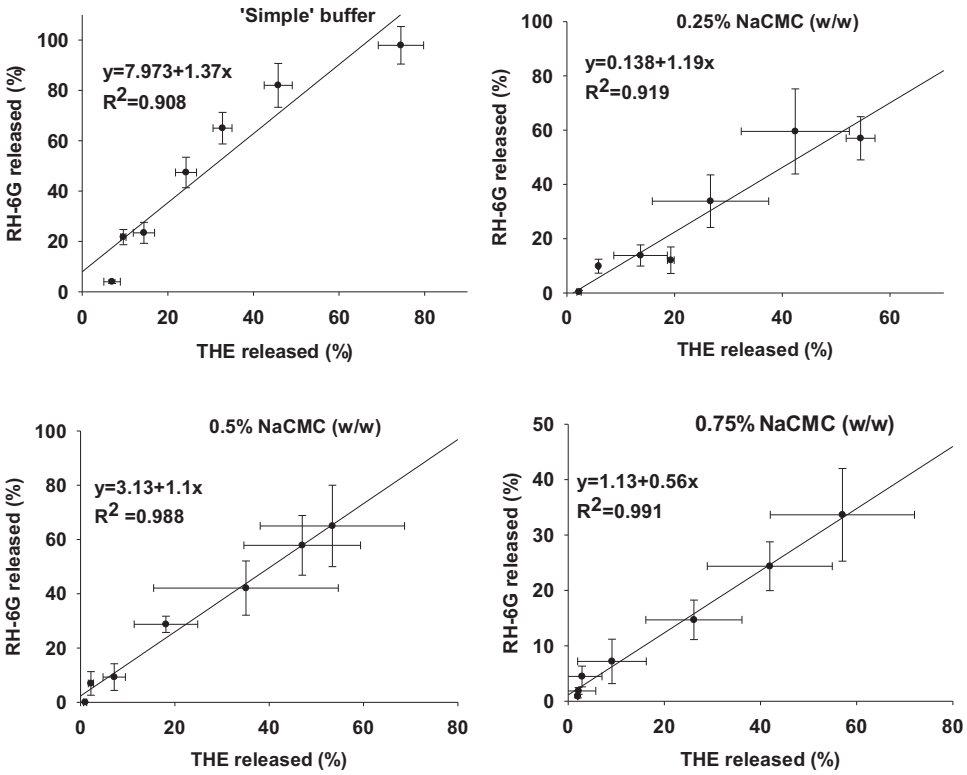

Fig. 5. Correlation between theophylline (THE) and rhodamine-6G (RH-6G) release data for SP2. (a) water, (b) 0.25%, (c) 0.50% and (d) 0.75% NaCMC (w/w). Standard deviation bars (±SD, $n = 6$).

substance (USP 32-NF 27, 2009). However, the rate of RH-6G dissolution may be faster than that for THE due to this difference in solubility values. This can lead to a fast saturation of the area around the blade (SP2 position) resulting in an intense fluorescence causing high grayscale values reflecting high release rates. As the dye reaches the upper region the concentration is decreased resulting in more normal values and better fitting with theophylline. An additional outcome is that in 'simple' buffer the dissolution profiles of THE obtained from the two sampling points were similar (f_2>50), but that was not the case in viscous media demonstrating the effect of viscosity on dissolution.

Furthermore, the values of m exponent (Table 3) showed that: (a) the sampling point can alter the m values, (b) the mechanism characterizing the release was the same for both compounds, since it was within the range of 0.5–0.89 (pH 1.0) and above one for pH 7.4. This implies that at pH 1.0, diffusion of the compound and polymer chain relaxation (anomalous non-Fickian) mainly affect the release of the compounds whereas at pH 7.4, high m values (>1) are typical for hydrophilic matrices, in which high release rate occurs due to high solubility of the polymer (i.e., NaCMC) at this pH, leading to gel erosion. This is further evidence that PLIF data can also describe the release mechanism of a highly water soluble drug from a hydrophilic matrix.

The effect of media viscosity on the mean dissolution time (MDT) is presented in Table 3. The results showed that as the viscosity increases the MDT also increases. The value of MDT between the two techniques (i.e. USP and PLIF) was not statistically significant (p > 0.05) at each experimental condition.

A linear correlation between THE and RH-6G release data was achieved for SP2 (Fig. 5). It was found that the average concentration of the drug obtained from conventional technique was in good correlation with the mean concentration of the dye for the same time intervals. The correlation plots were characterized by the coefficient of correlation values 0.908, 0.919, 0.988 and 0.991 for the 'simple buffer' (pH 7.4), 0.25%, 0.5% and 0.75% NaCMC (w/w), respectively.

3.4. Gel layer strength measurements

Previously researchers have carried out compression analysis experiments on hydrophilic matrices (Conti et al., 2007a; Ochoa et al., 2005; Yang et al., 1998) in order to make a correlation between the thickness and the strength of the tablet gel layer with the dissolution profiles of matrix tablet. Compression experiments performed in this work gave information about: (1) the gel layer strength (Fig. 6a), which is the measurement of the slope of the texture analysis curves (force vs probe penetration distance), (2) gel layer thickness (Fig. 6b) of NaCMC matrix at the two pH values under which the dissolution experiments were conducted and (3) the corresponding dissolution profile of THE (Fig. 6c). The gel strength of the hydrophilic matrix was stronger at pH 1.0 compared to the strength obtained at pH 7.4. In contrast the gel layer thickness was bigger at pH 7.4 compared to pH 1.0. This explains why the release rate of THE at pH 7.4 was higher (Fig. 6c) compared to pH 1.0. The hydration of the hydrophilic matrix was faster at pH 7.4 which is indicated by a significant increase of gel layer thickness of about 4 times within 5.5 hours compared to 2.5 times in case of pH 1.0. As a further consequence of fast hydration, the concentration of the polymer (i.e., NaCMC) within the gel layer is decreased leading to lower gel strength (Zuleger et al., 2002). It has been

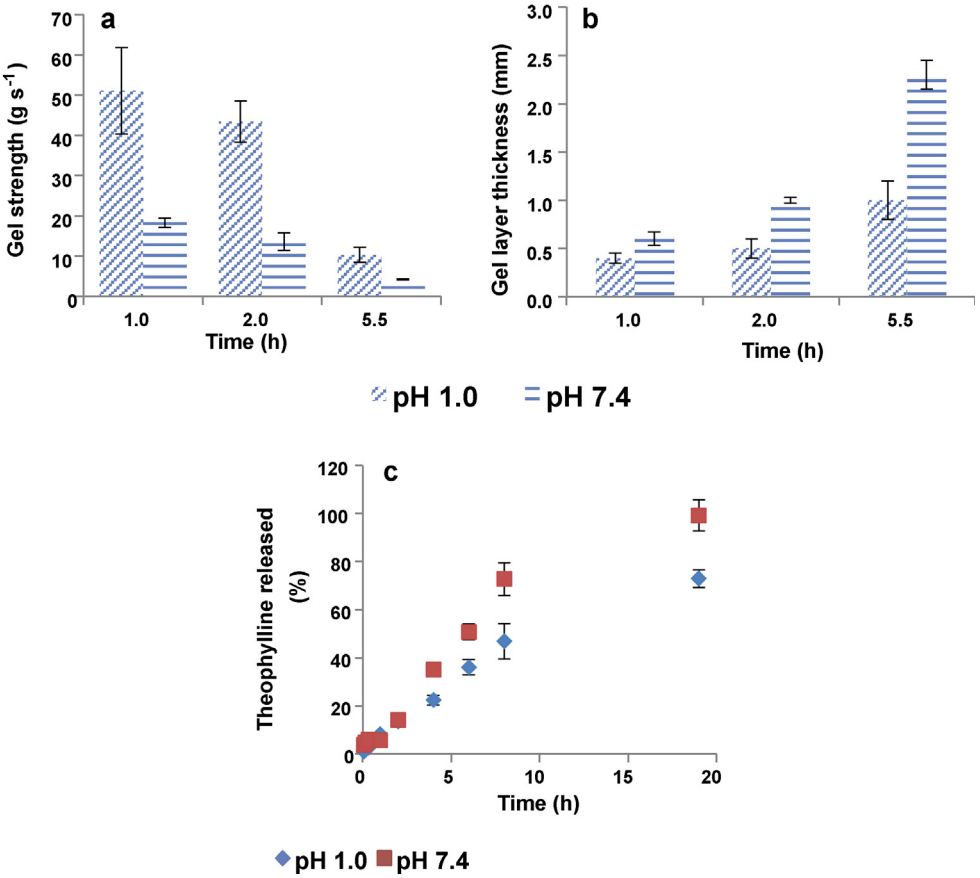

Fig. 6. Effect of pH on the gel layer strength (a) and thickness (b) as well as on the dissolution profile of THE (c). Standard deviation bars for gel strength and thickness (n = 6) and for dissolution profile of THE (n = 6).

reported that the drug release is increased as the gel thickness increases and the slope of force-penetration curve decreases (Ochoa et al., 2005). At pH 1.0 NaCMC is not soluble which may affect the hydration and subsequently the dissolution of the drug in the gel layer. In addition, the insufficient hydration at pH 1.0 results in the formation of a stronger gel layer (50–10 g s^{-1}) at pH 1.0 compared to pH 7.4 (19–4 g s^{-1}). This implies that the drug release mechanism is mainly due to the diffusion through the thick gel layer and no due to the erosion; since the erosion of the gel layer requires sufficient hydration of the polymer chains in order to reach the disentanglement concentration where the macromolecules begin to detach from the swollen matrix (Zuleger et al., 2002). The same conclusion has been made with regard to the release mechanism of THE at pH 1.0 by the release kinetics analysis based on m exponent values obtained after fitting the dissolution data using Korsmeyer-Peppas model. However, it has to point out that other factors such as high loadings (e.g., 50%) of water soluble drugs as well as hydrophilic additives (i.e., potato starch which is used in this study) may also have an impact on swelling behaviour and gel layer texture properties (Mitchell et al., 1993a; Zuleger et al., 2002) and hence on drug release. Nevertheless, the high drug loading in the current dosage form might also alter the release rate due to the increased porosity which leads to a fast release rate (Maderuelo et al., 2011) and which is not linked to the lower hydration at pH 1.0 compared to pH 7.4. Furthermore, burst release can occur at pH 1.0 since the gel hydration rate is slower and the drug molecules present at the surface of the dosage form can easily dissolve and pass into the medium (Conti et al., 2007a). Hence, these additional factors might explain why there was no a difference between the release profile of THE at two pH values (Fig. 6c) especially at the first two hours whilst the differences in gel thickness and strength were remarkable. Finally, there was no effect on the gel layer thickness and gel strength with the addition of RH-6 G in dosage form.

4. Conclusions

In this paper, the dissolution profile of a fluorescent dye Rhodamine 6G (RH-6G) released from a hydrophobic matrix tablet has been determined in a USP 2 mini vessel using PLIF. The profiles determined have been compared with results obtained using Theophylline (THE), a highly soluble drug.

The dissolution profiles of both RH-6G and THE were found to be statistically similar: a highly linear correlation was determined between the release data of the drug and the dye ($R^2 > 0.9$). Thus, RH-6G is an appropriate probe to mimic the release profile of a highly soluble drug.

Using viscous media, segregated zones were identified in the vessel, where high amounts of dye accumulated on the bottom of the vessel. This is due to highly inhomogeneous mixing intensities across the vessel resulting in non-uniform distribution of the dye. Analysis of PLIF images using MATLAB showed that for a given time, the concentration of RH-6G around the impeller was always higher in all experimental fluids compared to the upper region of the USP 2 mini vessel. This time delay for the released dye-drug to reach the upper zone of the dissolution apparatus leads to different release rates when different sampling points are used for generating the dissolution profile of the targeted drug.

The proof of concept that the dissolution profile of the fluorescent dye matches that of a common drug allows prediction of the performance of the dissolution test and thus guidelines in terms of sampling point and possible variance of the drug dissolution data obtained. The PLIF images showed better uniformity of the dye distribution above the blade and close to the wall. Thus, based on this analysis, positioning the cannula within this zone could minimize the variance of the dissolution data. Nevertheless, due to the design of the USP 2 there will be always limitations on the mixing performance and hence on the reproducibility of the dissolution data. These are critical and important results for practitioners using the device.

Further work has to be done on utilizing the current PLIF method for different BSC class drugs; provided that the proper dye has been selected. This is of great importance especially for low water soluble drugs, where the low amounts dissolved in viscous media could lead to even higher variance on the dissolution data generated with the conventional sampling technique.

Acknowledgement

Kostas Stamatopoulos is sponsored by an EPSRC DTG studentship at the School of Chemical Engineering, the University of Birmingham.

References

Bai, G., Wang, Y., Armenante, P.M., 2011. Velocity profiles and shear strain rate variability in the USP dissolution testing apparatus 2 at different impeller agitation speeds. Int. J. Pharm. 403, 1–14.
Baxter, J.L., Kukura, J., Muzzio, F.J., 2005a. Hydrodynamics-induced variability in the USP apparatus II dissolution test. Int. J. Pharm. 292, 17–28.
Baxter, J.L., Kukura, J., Muzzio, F.J., 2005b. Shear-induced variability in the United States pharmacopeia apparatus 2: modifications to the existing system. AAPS J. 7, E857–E864.
Bocanegra, L.M., Morris, G.J., Jurewicz, J.T., Mauger, J.W., 1990. Fluid and particle laser doppler velocity measurements and mass transfer predictions for the usp paddle method dissolution apparatus. Drug Dev. Ind. Pharm. 16, 1441–1464.
Brazel, C.S., Peppas, N.A., 1999. Mechanisms of solute and drug transport in relaxing, swellable, hydrophilic glassy polymers. Polymer 40, 3383–3398.
Bruchhausen, M., Guillard, F., Lemoine, F., 2005. Instantaneous measurement of two-dimensional temperature distributions by means of two-color planar laser induced fluorescence (PLIF). Exp. Fluids 38, 123–131.
Conti, S., Maggi, L., Segale, L., Ochoa Machiste, E., Conte, U., Grenier, P., Vergnault, G., 2007a. Matrices containing NaCMC and HPMC: 1. Dissolution performance characterization. Int. J. Pharm. 333, 136–142.
Conti, S., Maggi, L., Segale, L., Ochoa Machiste, E., Conte, U., Grenier, P., Vergnault, G., 2007b. Matrices containing NaCMC and HPMC: 2. Swelling and release mechanism study. Int. J. Pharm. 333, 143–151.
Costa, P., Lobo, J.M.S., 2001. Influence of dissolution medium agitation on release profiles of sustained-release tablets. Drug Dev. Ind. Pharm. 27, 811–817.
Ebube, N.K., Hikal, A.H., Wyandt, C.M., Beer, D.C., Miller, L.G., Jones, A.B., 1997. Sustained release of acetaminophen from heterogeneous matrix tablets: influence of polymer ratio, polymer loading, and co-active on drug release. Pharm. Dev. Technol. 2, 161–170.
Ford, J.L., Rubinstein, M.H., McCaul, F., Hogan, J.E., Edgar, P.J., 1987. Importance of drug type, tablet shape and added diluents on drug release kinetics from hydroxypropylmethylcellulose matrix tablets. Int. J. Pharm. 40, 223–234.
Gabriele, A., Nienow, A.W., Simmons, M.J.H., 2009. Corrigendum to "Use of angle resolved PIV to estimate local specific energy dissipation rates for up- and down-pumping pitched blade agitators in a stirred tank. Chem. Eng. Sci. 64, 126–143 Chemical Engineering Science 64, 4196.
Garbacz, G., Golke, B., Wedemeyer, R.S., Axell, M., Soderlind, E., Abrahamsson, B., Weitschies, W., 2009. Comparison of dissolution profiles obtained from nifedipine extended release once a day products using different dissolution test apparatuses. Eur. J. Pharm. Sci. 38, 147–155.
Ghori, M., Šupuk, E., Conway, B., 2015. Tribo-electrification and powder adhesion studies in the development of polymeric hydrophilic drug matrices. Materials 8, 1482–1498.
Gray, V., Kelly, G., Xia, M., Butler, C., Thomas, S., Mayock, S., 2009. The Science of USP 1 and 2 dissolution: present challenges and future relevance. Pharm. Res. 26, 1289–1302.
Hiremath, P.S., Saha, R.N., 2008. Oral controlled release formulations of rifampicin. Part II: effect of formulation variables and process parameters on in vitro release. Drug Deliv. 15, 159–168.
Khanvilkar, K.H., Huang, Y., Moore, A.D., 2002. Influence of hydroxypropyl methylcellulose mixture, apparent viscosity, and tablet hardness on drug release using a 2(3) full factorial design. Drug Dev. Ind. Pharm. 28, 601–608.
Klein, S., Shah, V.P., 2008. A standardized mini paddle apparatus as an alternative to the standard paddle. AAPS PharmSciTech 9, 1179–1184.
Korsmeyer, R.W., Gurny, R., Doelker, E., Buri, P., Peppas, N.A., 1983. Mechanisms of solute release from porous hydrophilic polymers. Int. J. Pharm. 15, 25–35.
Kukura, J., Arratia, P.E., Szalai, E.S., Muzzio, F.J., 2003. Engineering tools for understanding the hydrodynamics of dissolution tests. Drug Dev. Ind. Pharm. 29, 231–239.
Kukura, J., Baxter, J.L., Muzzio, F.J., 2004. Shear distribution and variability in the USP Apparatus 2 under turbulent conditions. Int. J. Pharm. 279, 9–17.

Law, A.W.-K., Wang, H., 2000. Measurement of mixing processes with combined digital particle image velocimetry and planar laser induced fluorescence. Exp. Therm. Fluid Sci. 22, 213–229.
Maderuelo, C., Zarzuelo, A., Lanao, J.M., 2011. Critical factors in the release of drugs from sustained release hydrophilic matrices. J. Controlled Release 154, 2–19.
Mauger, J.W., Brockson, R., De, S., Gray, V.A., Robinson, D., 2003. Intrinsic dissolution performance of USP apparatus 2 using modified salicylic acid calibrator tablets: proof of principle. Dissol. Technol. 10, 6.
Metzner, A.B., Otto, R.E., 1957. Agitation of non-Newtonian fluids. AIChE J. 3, 3–10.
Mitchell, K., Ford, J.L., Armstrong, D.J., Elliott, P.N.C., Hogan, J.E., Rostron, C., 1993a. The influence of drugs on the properties of gels and swelling characteristics of matrices containing methylcellulose or hydroxypropylmethylcellulose. Int. J. Pharm. 100, 165–173.
Mitchell, K., Ford, J.L., Armstrong, D.J., Elliott, P.N.C., Hogan, J.E., Rostron, C., 1993b. The influence of the particle size of hydroxypropylmethylcellulose K15M on its hydration and performance in matrix tablets. Int. J. Pharm. 100, 175–179.
Moroni, A., Ghebre-Sellassie, I., 1995. Application of poly(oxyethylene) homopolymers in sustained release solid formulations. Drug Dev. Ind. Pharm. 21, 1411–1428.
Ochoa, L., Igartua, M., Hernandez, R.M., Gascon, A.R., Pedraz, J.L., 2005. Preparation of sustained release hydrophilic matrices by melt granulation in a high-shear mixer. J. Pharm. Pharm. Sci. 8, 132–140.
Parojcic, J., Vasiljevic, D., Ibric, S., Djuric, Z., 2008. Tablet disintegration and drug dissolution in viscous media: paracetamol IR tablets. Int. J. Pharm. 355, 93–99.
Qureshi, S.A., McGilveray, I.J., 1999. Typical variability in drug dissolution testing: study with USP and FDA calibrator tablets and a marketed drug (glibenclamide) product. Eur. J. Pharm. Sci. 7, 249–258.
Qureshi, S.A., Shabnam, J., 2001. Cause of high variability in drug dissolution testing and its impact on setting tolerances. Eur. J. Pharm. Sci. 12, 271–276.
Radwan, A., Amidon, G.L., Langguth, P., 2012. Mechanistic investigation of food effect on disintegration and dissolution of BCS class III compound solid formulations: the importance of viscosity. Biopharm. Drug Dispos. 33, 403–416.
Ranga Rao, K.V., Padmalatha Devi, K., 1988. Swelling controlled-release systems: recent developments and applications. Int. J. Pharm. 48, 1–13.
van Cruyningen, I., Lozano, A., Hanson, R.K., 1990. Quantitative imaging of concentration by planar laser-induced fluorescence. Exp. Fluids 10, 41–49.
Yang, L., Fassihi, R., 1996. Zero-order release kinetics from a self-correcting floatable asymmetric configuration drug delivery systemxd. J. Pharm. Sci. 85, 170–173.
Yang, L., Johnson, B., Fassihi, R., 1998. Determination of continuous changes in the gel layer thickness of poly(ethylene oxide) and hpmc tablets undergoing hydration: a texture analysis study. Pharm. Res. 15, 1902–1906.
Zuleger, S., Fassihi, R., Lippold, B.C., 2002. Polymer particle erosion controlling drug release. II. Swelling investigations to clarify the release mechanism. Int. J. Pharm. 247, 23–37.
Zuleger, S., Lippold, B.C., 2001. Polymer particle erosion controlling drug release. I. Factors influencing drug release and characterization of the release mechanism. Int. J. Pharm. 217, 139–152.